Stationary solutions for the 1+1 nonlinear Schrödinger equation modeling repulsive Bose-Einstein condensates in small potentials

Kristina Mallory and Robert A. Van Gorder

Phys. Rev. E **88**, 013205 — Published 29 July 2013

DOI: 10.1103/PhysRevE.88.013205

Stationary solutions for the $1+1$ nonlinear Schrödinger equation modeling repulsive Bose-Einstein condensates in small potentials

Kristina Mallory and Robert A. Van Gorder*
Department of Mathematics, University of Central Florida, Orlando, FL 32816-1364 USA
**Corresponding author. Email: rav@knights.ucf.edu*

Stationary solutions for the $1+1$ cubic nonlinear Schrödinger equation modeling repulsive Bose-Einstein condensates (BEC) in a small potential are obtained through a form of nonlinear perturbation. In particular, for sufficiently small potentials, we determine the perturbation theory of stationary solutions, by use of an expansion in Jacobi elliptic functions. This idea was explored before in order to obtain exact solutions [J. C. Bronski, L. D. Carr, B. Deconinck, and J. N. Kutz, Phys. Rev. Lett. 86 (2001) 1402], where the potential itself was fixed to be a Jacobi elliptic function, thereby reducing the nonlinear ODE into an algebraic equation, (which could be easily solved). However, in the present paper, we outline the perturbation method for completely general potentials, assuming only that such potentials are locally small. We do not need to assume that the nonlinearity is small, as we perform a sort of nonlinear perturbation by allowing the zeroth-order perturbation term to be governed by a nonlinear equation. This allows us to consider even poorly behaved potentials, so long as they are bounded locally. We demonstrate the effectiveness of this approach by considering a number of specific potentials: for the simplest potentials, we recover results from the literature, while for more complicated potentials, our results are new. Dark soliton solutions are constructed explicitly for some cases, and we obtain the known one-soliton tanh-type solution in the simplest setting for the repulsive BEC. Note that we limit our results to the repulsive case; similar results can be obtained for the attractive BEC case.

Keywords: cubic nonlinear Schrödinger equation; Bose-Einstein condensate; perturbation theory; Jacobi elliptic function

PACS numbers: 05.45.Yv 04.25.Nx 05.30.Jp

I. INTRODUCTION

Recently, the cubic form of the nonlinear Schrödinger equation (NLS) has been used to model the dilute-gas Bose-Einstein condensate (BEC) in the quasi-one-dimensional regime [1]. In such a model, the potential can be used to model a trap. A variety of potentials have been proposed for BECs [2], depending upon the specific application addressed.

Exact solutions for such cubic NLS equations have been obtained for several potentials, such as the Kronig-Penney potential [3] and the Jacobi elliptic function potential of the sn type [4]. Exact solutions for the latter case took the form of Jacobi elliptic functions of type sn, cn, or dn, depending on the values of the model parameter. In the limit of a sinusoidal potential, those solutions are one possible model for a dilute gas Bose-Einstein condensate trapped in a standing light wave. BECs trapped in a standing light wave have been used to study or have been proposed to study
(i) phase coherence [5];
(ii) matter-wave diffraction [6];
(iii) quantum logic [7];
(iv) matter-wave transport [8].

Let $V(x)$ be a potential function which has been normalized so that $\max V(x) = 1$. Then, the $n+1$ cubic nonlinear Schrödinger equation (NLS) (also referred to as the Gross-Pitaevskii model in some literature [9]) with small potential reads

$$i\hbar\Psi_t = \left(-\frac{\hbar^2}{2m}\nabla^2 + \epsilon V(\mathbf{r}) + g|\Psi|^2\right)\Psi\,. \tag{1}$$

For our interests, we shall be concerned with the $1+1$ model

$$i\hbar\Psi_t = -\frac{\hbar^2}{2m}\Psi_{xx} + \epsilon V(x)\Psi + g|\Psi|^2\Psi\,, \tag{2}$$

where $g > 0$. Our focus, then, shall be on the repulsive case. Results for the attractive case will follow similarly.

Concerning BECs, stationary solutions to the one-dimensional nonlinear Schrödinger equation under box and periodic boundary conditions were considered analytically for the repulsive [10] and attractive [11] cases. The stability of repulsive BECs in periodic potentials was previously discussed in [12]. BECs in a ring-shaped trap with a nonlinear double-well potential were recently considered [13]. Regarding the PT-symmetric case, a model of a PT-symmetric BEC in a δ-function double-well potential was also recently considered [14]. Further results on multiwell potentials have been given [15].

While there have been numerical and some exact or analytical studies on specific potentials, a perturbation method for arbitrary potentials has not been proposed. As for solutions in the literature, if $\epsilon = 0$ we effectively have the free particle potential and we recover an exact solution. For an appropriate elliptic index, this exact solution reduces to the standard dark soliton solution.

For a constant potential, $V(x) = \lambda$, we effectively have a mass-shifted variant of the zero-potential case. Modern approaches have been developed for more complicated potentials. Since the $\epsilon = 0$ case results naturally in Jacobi elliptic functions, it is reasonable to assume a potential which can be expressed as such a function. This was done in [4] as a model of a trapping potential generated by a standing light wave. Naturally, since such a potential is mathematically consistent with the form of the $\epsilon = 0$ solution, the authors were able to recover elegant exact solutions. Other potentials were considered in [4], where a mix of analytical and numerical results were given. This brings about a natural question: For how many potentials can we exactly, or at the very least analytically, solve the stationary states of the model (2)? While the choice of a Jacobi elliptic potential is an example of a complicated potential giving an exact solution, this is more due to luck, since the natural unperturbed solution is itself a Jacobi elliptic function.

In the present paper, we shall develop a perturbation theory of stationary solutions to the $1 + 1$ model (2). As seen before, the lowest order term will be governed by a non-linear ODE, resulting in a Jacobi elliptic function (a type of non-linear special function). If the elliptic index is properly selected, this will give a dark soliton type solution at $\epsilon = 0$. For other values of the elliptic index, we recover a space-periodic stationary solution at $\epsilon = 0$. So, for small ϵ, we carry out perturbation around these non-linear special functions, effectively calculating the corrections due to a small potential. In order to better illustrate the results, we consider NLS equations with a variety of potentials. Exact solutions can be obtained when $V(x) = 0$, $V(x) = V_0$ (a constant), or when $V(x)$ is a specific function of Jacobi elliptic functions. For other situations, the first or even second order perturbation terms are constructed; examples of cases we consider include the δ function potential, the linear potential, the harmonic potential, the Coulomb potential, the Morse potential and the quantum pendulum potential. These potentials are selected more to demonstrate the range of solutions possible; indeed, some specific potentials will be more physically relevant for the study of BECs than others.

The primary benefit to our approach is that it allows for fairly general forms of the potential function. That is to say, for sufficiently well-behaved functions $V(x)$, we can calculate the first-order perturbation theory for the stationary solutions to the model (2) given potentials of the form $\epsilon V(x)$. Since we consider a type of non-linear perturbation (the zeroth-order term is governed by a non-linear differential equation), we need not assume a small amplitude solution, requiring only that the higher order corrections are small. Hence, the perturbation method presented here is applicable for a wide variety of scenarios.

II. STATIONARY SOLUTION AND ORDER ZERO PERTURBATION THEORY

We begin by introducing the stationary solution

$$\Psi(x,t) = 2\hbar\sqrt{\frac{m}{g}}\exp\left(-4i\hbar m t\right)\psi(x)\,. \tag{3}$$

This reduces (2) to the eigenvalue problem

$$\psi'' = -\psi + \psi^3 + \epsilon U(x)\psi\,, \tag{4}$$

where we define the non-dimensional potential U by

$$U(x) = \frac{1}{2\hbar\sqrt{mg}}V(x)\,. \tag{5}$$

Now, integrating the eigenvalue problem (4) gives

$$\psi'^2 = K^2 - \psi^2 + \frac{1}{2}\psi^4 + 2\epsilon\int_0^x U(y)\psi(y)\psi'(y)\,\mathrm{d}y\,, \tag{6}$$

which is not exactly integrable when $U \neq 0$. However, observe that when $\epsilon = 0$, the equation is, in fact, exactly integrable. If we consider a perturbation solution of the form

$$\psi(x) = \psi_0(x) + \epsilon\psi_1(x) + \epsilon^2\psi_2(x) + \cdots\,, \tag{7}$$

then we may obtain the perturbative stationary solution to the $1 + 1$ GP equation

$$\begin{aligned}\Psi(x,t) &= \Psi_0(x,t) + \epsilon\Psi_1(x,t) + \epsilon^2\Psi_2(x,t) + \cdots \\ &= 2\hbar\sqrt{\frac{m}{g}}e^{-4i\hbar m t}(\psi_0(x) + \epsilon\psi_1(x) + \epsilon^2\psi_2(x) + \cdots)\end{aligned} \tag{8}$$

Now, utilizing the perturbation solution (7), we see that $\psi_0(x)$ satisfies

$$\psi_0'^2 = K^2 - \psi_0^2 + \frac{1}{2}\psi_0^4\,. \tag{9}$$

Thus, our solution to (9), with the assumed initial condition $\psi_0(0) = 0$, reads

$$\psi_0(x) = K\ \mathrm{sn}\left(\frac{\sqrt{2-K^2}}{\sqrt{2}}x + x_0, \frac{K}{\sqrt{2-K^2}}\right)\,, \tag{10}$$

where $\mathrm{sn}(x,\nu)$ is the Jacobi elliptic sn function with index ν and x_0 is an arbitrary constant which has the effect of shifting the solution. Note that $\psi_0'(0) = K$, which clearly follows in the context of equation (9). In the special case where $\nu = 1$ (corresponding to $K^2 = 1$), we make use of the identity $\mathrm{sn}(x,1) = \tanh(x)$ to obtain

$$\psi_0(x) = \tanh\left(\frac{x}{\sqrt{2}} + x_0\right)\,. \tag{11}$$

We shall frequently revisit the $K^2 = 1$ case, as it will greatly simplify some calculations. Such solutions, based

around the tanh-solution, will be perturbations of dark soliton solutions.

As it turns out, a number of equations in mathematical physics naturally admit solutions in terms of Jacobi elliptic functions, particularly when we consider stationary states [16]. Regarding the construction of perturbation expansions for such solutions then, due either to added non-linearity or complicated potentials, it seems quite reasonable to construct these perturbation theories in terms of the Jacobi elliptic functions.

III. PERTURBATION SOLUTIONS FOR GENERAL POTENTIALS

Let us now compute the higher order terms in the perturbation expansion (7) for the general potential $U(x)$. Notice we will utilize ${\psi_0}'(x)$ as the function given by

$$ {\psi_0}'(x) = \sqrt{K^2 - {\psi_0}^2 + \frac{1}{2}{\psi_0}^4}, \tag{12} $$

where $\psi_0(x)$ is our previously determined function (10). Placing (7) into our equation (6), we obtain $\psi_1(x)$ via the linear differential equation represented in the first order term in ϵ

$$ \begin{aligned} {\psi_1}'(x) = \frac{1}{{\psi_0}'(x)} \Big[\left({\psi_0}^3(x) - \psi_0(x)\right) \psi_1(x) \\ + \int_0^x U(y)\psi_0(y){\psi_0}'(y)\,\mathrm{d}y \Big] . \end{aligned} \tag{13} $$

Satisfying $\psi_1(0) = 0$, our first-order term becomes

$$ \psi_1(x) = \int_0^x \frac{\int_0^y U(z)\psi_0(z){\psi_0}'(z)\,\mathrm{d}z}{{\psi_0}'(y)} \mathrm{e}^{-\int_y^x \frac{\psi_0(z) - {\psi_0}^3(z)}{{\psi_0}'(z)}\,\mathrm{d}z}\,\mathrm{d}y . \tag{14} $$

Notice we may greatly simplify the integrating factor in our solution $\psi_1(x)$ by rewriting our integrand as

$$ \begin{aligned} \int_0^x \frac{\left(\psi_0(y) - {\psi_0}^3(y)\right){\psi_0}'(y)}{{{\psi_0}'}^2(y)}\,\mathrm{d}y \\ = -\frac{1}{2}\ln(K^2 - {\psi_0}^2(x) + \frac{1}{2}{\psi_0}^4(x)), \end{aligned} $$

thereby reducing our integrating factor to precisely

$$ \begin{aligned} \mathrm{e}^{\frac{1}{2}\ln\left(K^2 - {\psi_0}^2(x) + \frac{1}{2}{\psi_0}^4(x)\right)} &= \sqrt{K^2 - {\psi_0}^2(x) + \frac{1}{2}{\psi_0}^4(x)} \\ &= {\psi_0}'(x) . \end{aligned} $$

This computation reduces our first-order solution given in (14) to

$$ \psi_1(x) = {\psi_0}'(x) \int_0^x \frac{\int_0^y U(z)\psi_0(z){\psi_0}'(z)\,\mathrm{d}z}{{{\psi_0}'}^2(y)}\,\mathrm{d}y . \tag{15} $$

Now, in a similar manner, we may obtain our second-order solution $\psi_2(x)$ by solving the relevant ODE subject to $\psi_2(0) = 0$, which gives

$$ \psi_2(x) = {\psi_0}'(x) \int_0^x \frac{M_1(y)}{{{\psi_0}'}^2(y)}\,\mathrm{d}y , \tag{16} $$

where

$$ \begin{aligned} M_1(y) = \int_0^y U(z)\left(\psi_0(z){\psi_1}'(z) + \psi_1(z){\psi_0}'(z)\right)\,\mathrm{d}z \\ + \frac{3}{2}{\psi_0}^2(y){\psi_1}^2(y) - \frac{1}{2}\left({\psi_1}^2(y) + {{\psi_1}'}^2(y)\right) . \end{aligned} $$

With this, we have determined the second order perturbation theory for the stationary solution under a general potential $U(x)$. In the next section, we shall utilize our general solution to consider stationary solutions under specific forms of $U(x)$ and to explore the resulting solutions.

IV. SOLUTIONS FOR SPECIFIC POTENTIALS

We now turn our attention toward a number of examples of specific potentials in order to demonstrate the method. For a number of potentials, we demonstrate the analytical construction of the perturbation solutions for the dark soliton case. The corresponding results for the sn-waves can also be constructed, but we omit such derivations as they are tedious. For all non-trivial cases considered, we provide plots of the scaled density $\frac{g}{4\hbar^2 m}|\Psi(x,t)|^2 = |\psi(x)|^2$ in order to demonstrate the influence of each potential on the obtained solutions. As will be remarked later, the perturbation results are in agreement with numerical simulations, for sufficiently small ϵ.

A. Free particle

Note that the free particle solution, corresponding to $U(x) \equiv 0$, is exactly determined by $\psi_0(x)$. As such,

$$ \begin{aligned} \Psi(x,t) = 2\hbar\sqrt{\frac{m}{g}} K \exp\left(-4i\hbar m t\right) \\ \times\ \mathrm{sn}\left(\frac{\sqrt{2-K^2}}{\sqrt{2}}x + x_0, \frac{K}{\sqrt{2-K^2}}\right) \end{aligned} \tag{17} $$

is a family of exact solutions (indexed by $K > 0$) for the free particle. If we impose the condition $|\Psi(x,t)| \to 2\hbar\sqrt{\frac{m}{g}}$ as $x \to \infty$ and take $K^2 = 1$, then we have the exact solution

$$ \Psi(x,t) = 2\hbar\sqrt{\frac{m}{g}} \exp\left(-4i\hbar m t\right) \tanh\left(\frac{x}{\sqrt{2}}\right) \tag{18} $$

for the free particle. Note that this is qualitatively distinct from the Hartree solution $\Psi(\mathbf{r}) \sim e^{i\mathbf{n}\cdot\mathbf{r}}$. This solution is the standard one-soliton solution for repulsive BEC. In what follows, when we assume $K^2 = 1$, we shall obtain perturbations of this soliton solution. The first and higher order perturbation theories are simply corrections to this soliton solution due to the presence of a small potential.

B. Constant potential

Let us consider the constant potential $U(x) = \lambda$. With this potential, (1) models a vortex filament in an almost ideal Bose gas [9]. Independent of $U(x)$, $\psi_0(x)$ remains, as given in (10),

$$\psi_0(x) = K\ \mathrm{sn}\left(\frac{\sqrt{2-K^2}}{\sqrt{2}}x + x_0, \frac{K}{\sqrt{2-K^2}}\right). \tag{19}$$

Next, applying this constant potential $U(x) = \lambda$ to $\psi_1(x)$, denoted by (15), enables our inner integral in $\psi_1(x)$ to be solved exactly as $\frac{\lambda}{2}\psi_0(x)^2$. For simplicity, we will proceed taking

$$a = \frac{\sqrt{2-K^2}}{\sqrt{2}} \qquad \text{and} \qquad b = \frac{K}{\sqrt{2-K^2}}. \tag{20}$$

Recalling

$$\frac{d}{\mathrm{d}x}\mathrm{sn}(ax,b) = a\mathrm{cn}(ax,b)\mathrm{dn}(ax,b), \tag{21}$$

where $\mathrm{cn}(ax,b) = \sqrt{1-\mathrm{sn}^2(ax,b)}$ and $\mathrm{dn}(ax,b) = \sqrt{1-b^2\mathrm{sn}^2(ax,b)}$ are Jacobi elliptic functions, we have

$$\begin{aligned}\psi_1(x) &= \frac{K\lambda}{2a}\mathrm{cn}(ax,b)\mathrm{dn}(ax,b)\int_0^x \frac{\mathrm{sn}^2(ay,b)}{\mathrm{cn}^2(ay,b)\mathrm{dn}^2(ay,b)}\mathrm{d}y \\ &= \frac{K\lambda\mathrm{cn}(ax,b)\mathrm{dn}(ax,b)}{2a^2}\left[\frac{\mathrm{sn}(ax,b)[2b^2\mathrm{sn}^2(ax,b)-b^2-1]}{(1-b^2)^2[\mathrm{sn}^2(ax,b)-1]}\right. \\ &\quad \left. + \frac{ax}{1-b^2} - \frac{2}{(1-b^2)^2}E(\mathrm{sn}(ax,b),b)\right].\end{aligned} \tag{22}$$

Here $E(x,b)$ denotes the incomplete elliptic integral of the second kind.

Now, utilizing the simple condition where $K^2 = 1$, $\psi_1(x)$ becomes

$$\begin{aligned}\psi_1(x) &= \frac{\lambda}{8}\tanh\left(\frac{x}{\sqrt{2}}\right)\left(2\cosh^2\left(\frac{x}{\sqrt{2}}\right)-1\right) \\ &\quad + \frac{\lambda}{16}\left(1-\tanh^2\left(\frac{x}{\sqrt{2}}\right)\right)\ln\left(\frac{1-\tanh\left(\frac{x}{\sqrt{2}}\right)}{\tanh\left(\frac{x}{\sqrt{2}}\right)+1}\right).\end{aligned} \tag{23}$$

Of course, since the potential is constant, we may directly obtain the exact solution by solving

$$\psi'^2 = K^2 - (1-\epsilon\lambda)\psi^2 + \frac{1}{2}\psi^4 \tag{24}$$

and obtaining

$$\psi(x) = K\mathrm{sn}\left(\frac{\sqrt{2-K^2-2\epsilon\lambda}}{\sqrt{2}}x + x_0, \frac{K}{\sqrt{2-K^2-2\epsilon\lambda}}\right). \tag{25}$$

This exact solution agrees qualitatively with the perturbation solution when ϵ is small. Taking $K^2 = 1-\epsilon\lambda$, we recover the dark soliton

$$\psi(x) = \sqrt{1-\epsilon\lambda}\tanh\left(\frac{\sqrt{1-\epsilon\lambda}}{2}x\right). \tag{26}$$

C. delta potential

The δ potential is given by $U(x) = \lambda\delta(x-x_0)$, where δ denotes the Dirac delta function, $\lambda \in \mathbb{R}$, and $x_0 \in \mathbb{R}$ is a constant. This potential arises in some applications [17]. Note also that the results we obtain here are similar for the double delta potential [18]. Additionally, the quantum Hall effect of bosons interacting through a delta potential has been considered previously [19].

With this choice of potential and $\psi_0(x)$ as written in (10), the inner integral in $\psi_1(x)$ becomes

$$\begin{aligned}\int_0^y U(z)\psi_0(z)\psi_0'(z)\mathrm{d}z &= \lambda\int_0^y \delta(z-x_0)\psi_0(z)\psi_0'(z)\mathrm{d}z \\ &= \lambda(H(y-x_0)+H(x_0)-1)\psi_0(x_0)\psi_0'(x_0),\end{aligned} \tag{27}$$

in which H denotes the Heaviside function

$$H(\eta) = \begin{cases} 0 & \text{if } \eta < 0, \\ 1 & \text{if } \eta \geq 0. \end{cases} \tag{28}$$

From here we find that

$$\begin{aligned}\psi_1(x) &= \sqrt{2}\lambda\psi_0(x_0)\psi_0'(x_0)\psi_0'(x) \\ &\quad \times \int_0^x \frac{H(y-x_0)+H(x_0)-1}{\psi_0'(y)^2}\mathrm{d}y.\end{aligned} \tag{29}$$

Considering the special case $K = 1$ and performing the required integration, we obtain

$$\begin{aligned}\psi_1(x) &= \frac{\sqrt{2}}{8}\lambda\tanh\left(\frac{x_0}{\sqrt{2}}\right)\mathrm{sech}^2\left(\frac{x_0}{\sqrt{2}}\right)\mathrm{sech}^2\left(\frac{x}{\sqrt{2}}\right) \\ &\quad \times [M_2(x)\left(H(x-x_0)-H(-x_0)+H(x_0)\right) \\ &\quad -M_2(x_0)\left(H(x-x_0)-H(-x_0)\right)],\end{aligned} \tag{30}$$

where

$$\begin{aligned}M_2(x) &= \sinh\left(\frac{x}{\sqrt{2}}\right)\cosh\left(\frac{x}{\sqrt{2}}\right)\left(2\cosh^2\left(\frac{x}{\sqrt{2}}\right)+3\right) \\ &\quad + \frac{3\sqrt{2}}{2}x.\end{aligned} \tag{31}$$

Some solutions are given in Fig. 1 for the $K = 1$ case: the dark soliton solutions. When $\lambda > 0$, the solutions

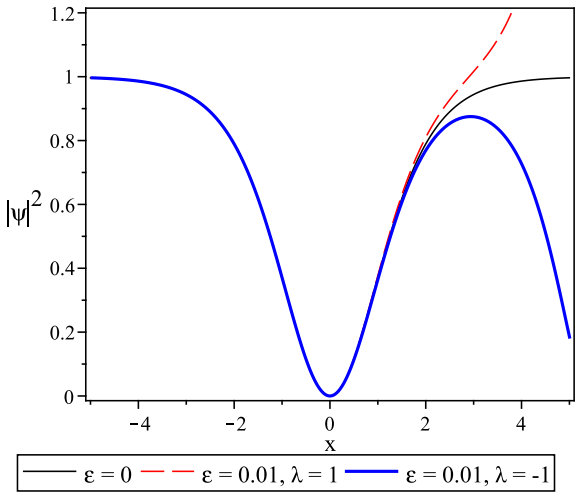

FIG. 1: (Color Online) Perturbations of the dark soliton solutions ($K = 1$) under the delta potential $U(x) = \lambda\delta(x - x_0)$. We fix $x_0 = 0$.

become unstable for large ϵ. In contrast, when $\lambda < 0$, the perturbed solutions exhibit oscillation past the point at which the impulse is placed. We have taken very small values of ϵ in our plots. For larger values, the solutions tend to either break down or become non-physical. For $x < x_0$, the solutions are invariant under perturbations due to this type of potential, since the effect of the perturbation is felt only for $x > x_0$. Therefore, when $x < x_0$ we maintain the dark soliton structure, whereas for $x > x_0$ this structure degenerates into an oscillatory branch, or a non-physical branch with blow-up, depending on the sign of λ.

D. Harmonic potential

Next we may examine the harmonic oscillator potential, $U(x) = \lambda x^2$ with $\lambda \in \mathbb{R}$. Harmonic potentials have been used as external potentials for BECs in a number of studies as they serve as a relatively accurate and simple model of a parabolic trap [20]. It should be noted that such potentials can be generalized to include time dependence [21], but this is beyond the scope of the present paper as such generalizations (in general) deny us of a stationary state of the kind we study here. Imposing the $K^2 = 1$ condition, $\psi_0(x)$ is given in (11). Let us define the function

$$
\begin{aligned}
M_3(x) = {} & \frac{\sqrt{2}x}{16}\left(e^{2\sqrt{2}x} + 8e^{\sqrt{2}x} + 12\ln 2 - 7\right) \\
& - \frac{x^2}{8}\left(2\sinh(\sqrt{2}x) - 3\right) - \frac{\sqrt{2}x^3}{12} - \frac{\ln(e^{\sqrt{2}x}+1)}{8} \\
& \times \left(8\sinh(2\sqrt{2}x) + \sinh(\sqrt{2}x) - 6\ \mathrm{dilog}(e^{\sqrt{2}x}+1)\right) \\
& + \frac{1}{16}\left[\pi^2 + 2\ln 2\sinh(2\sqrt{2}x) + (16\ln 2 - 2)\sinh(\sqrt{2}x)\right]
\end{aligned}
\tag{32}
$$

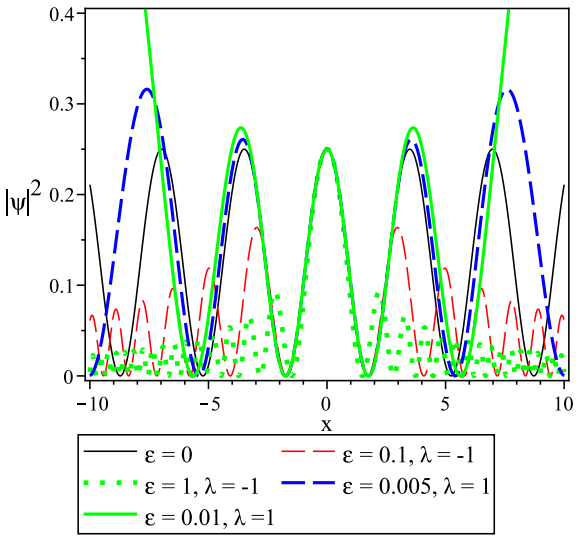

FIG. 2: (Color Online) Perturbations of the space-periodic sn-wave solution under the harmonic oscillator potential, which takes the quadratic form $U(x) = \lambda x^2$.

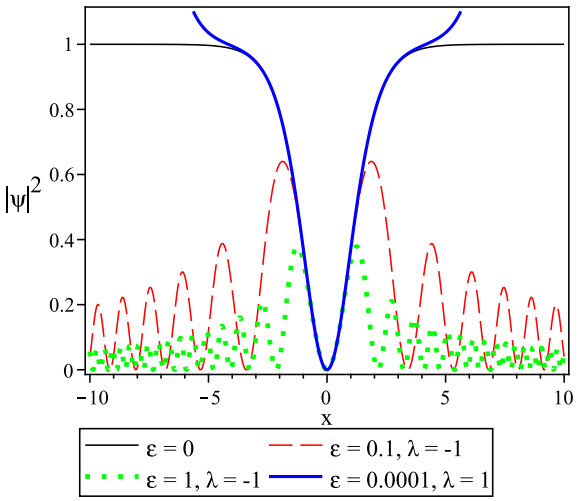

FIG. 3: (Color Online) Perturbations of the dark soliton solution corresponding to $K = 1$ under the harmonic oscillator potential, which takes the quadratic form $U(x) = \lambda x^2$.

so that the first order term $\psi_1(x)$ reads

$$
\psi_1(x) = \lambda\ \mathrm{sech}^2\left(\frac{x}{\sqrt{2}}\right) M_3(x)\,. \tag{33}
$$

In Fig. 2, we plot solutions which are perturbations of the sn-wave solution for the harmonic oscillator potential. Then, in Fig. 3, we plot several perturbation solutions corresponding to perturbations of the $K = 1/\sqrt{2}$ exact solution (the dark soliton). Under the perturbation due to the harmonic potential, the sn-wave solutions either amplify or de-amplify, depending on the sign of λ. When $\lambda < 0$, the solutions maintain their oscillatory nature, but tend toward zero as $|x|$ increases. Thus, the maximal density is found near the origin. The period of these

solutions decreases radially, and for large ϵ these solutions resemble solitary waves with radiation or chirp in the background. On the other hand, when $\lambda > 0$, the solutions oscillate yet increase in density as $|x|$ increases. These solutions are expected to be unstable for large ϵ, since the strong radial amplification is not physical. Regarding the perturbations of the dark solitons shown in Fig. 3, the solutions appear stable for $\lambda < 0$ and unstable for $\lambda > 0$. Indeed, even for $\epsilon = 10^{-3}$, the $\lambda > 0$ solutions demonstrate blow-up for large $|x|$. On the other hand, the $\lambda < 0$ perturbed solutions degenerate from the dark soliton into damped sn-type solutions with increasing ϵ, as can be seen from the density plots in Fig. 3. Again, the oscillations decay more rapidly with increasing ϵ.

For sake of demonstration, we have included $\epsilon = 1$ plots in Figs. 2-3. This solution was obtained numerically, since it is not in the perturbative regime. However, as we see here, it exhibits qualitative agreement with the perturbation results. It is worth mentioning that the perturbation solution for this and other potentials have been compared with numerical plots, and there is excellent agreement for sufficiently small ϵ.

E. Modified harmonic potential

There have been a number of modifications to the harmonic trap used in the literature [22]. One such potential is $U(x) = \lambda(x^2 + \beta/x^\alpha)$. Another useful potential is $U(x) = \lambda(x^2 + \beta\exp(-x^2))$. This latter potential is useful in that it avoids a singularity near the origin.

Using the potential $U(x) = \lambda(x^2 + \beta/x)$ (that is, $\alpha = 1$), we consider perturbations of the dark soliton in Fig. 4. When $\lambda < 0$, these solutions exhibit an asymmetry with respect to $x = 0$. When $\beta > 0$, most of the density is relegated to the $x < 0$ region, while when $\beta < 0$, most of the density is relegated to the $x > 0$ region. Like in the case of a pure harmonic potential, the density oscillates yet decreases radially away from $x = 0$. For these solutions, an increase in ϵ results in a decrease in the amplitude. In the case of $\lambda > 0$, the solutions become unstable at even small values of ϵ.

We next consider the potential $U(x) = \lambda(x^2 + \beta\exp(-x^2))$, and plot the perturbations of the sn-waves in Fig. 5, and perturbations of the dark soliton in Fig. 6. When $\lambda < 0$ and $\beta > 0$, the solutions behave like those in the pure harmonic potential, with the primary difference being an even more rapid decrease in the amplitude as $|x|$ is increased. However, all of these solutions still have maximal density at the origin. On the other hand, solutions corresponding to $\lambda < 0$ yet $\beta < 0$ have a double maximum in density (provided that ϵ is large enough), occurring symmetrically on both sides of $x = 0$. These solutions still decay in amplitude as $|x|$ increases, even more rapidly than their $\beta > 0$ counterparts. When $\lambda > 0$, we actually obtain bounded and apparently stable solutions for small enough ϵ. These solutions oscillate in density, yet the oscillations amplify as $|x|$ increases, until, for large enough $|x|$, the solutions decay.

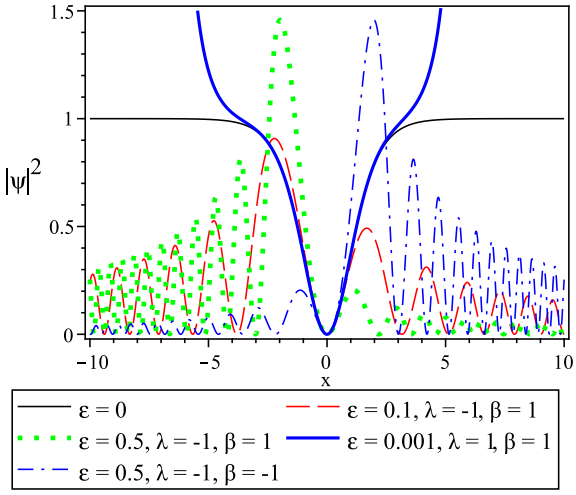

FIG. 4: (Color Online) Perturbations of the dark soliton solution corresponding to $K = 1$ under the modified harmonic oscillator potential $U(x) = \lambda x^2 + \beta/x$.

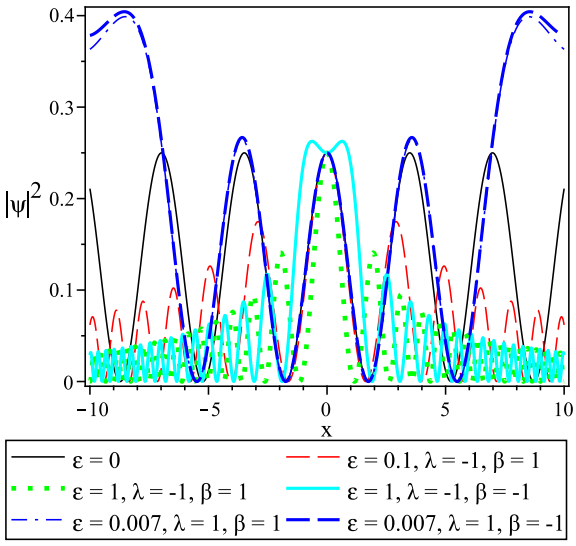

FIG. 5: (Color Online) Perturbations of the space-periodic sn-wave solution under the modified harmonic oscillator potential $U(x) = \lambda(x^2 + \beta\exp(-x^2))$.

Regarding the perturbations of the dark solitons, we find that $\lambda > 0$ perturbations are unstable, whereas for $\lambda < 0$ solutions oscillate in density and gradually decay, much like what we have seen earlier in the purely harmonic potential case. For small fixed ϵ, we find that the $\beta < 0$ solutions have higher central density than do the corresponding $\beta > 0$ solutions.

F. Morse potential: an asymmetric trap

Single well traps that are asymmetric are sometimes considered and can take a variety of forms. The

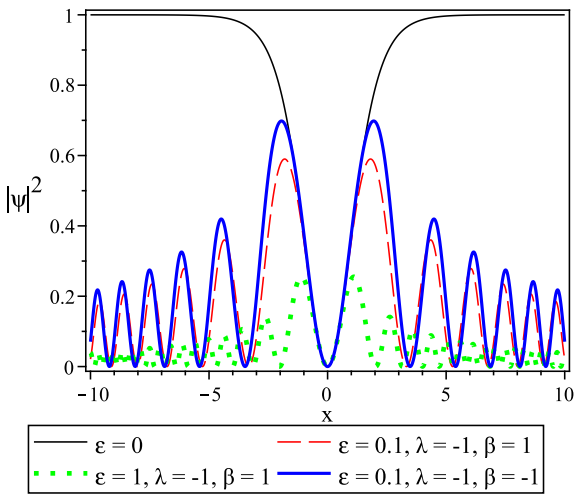

FIG. 6: (Color Online) Perturbations of the dark soliton solution corresponding to $K = 1$ under the modified harmonic oscillator potential $U(x) = \lambda(x^2 + \beta \exp(-x^2))$.

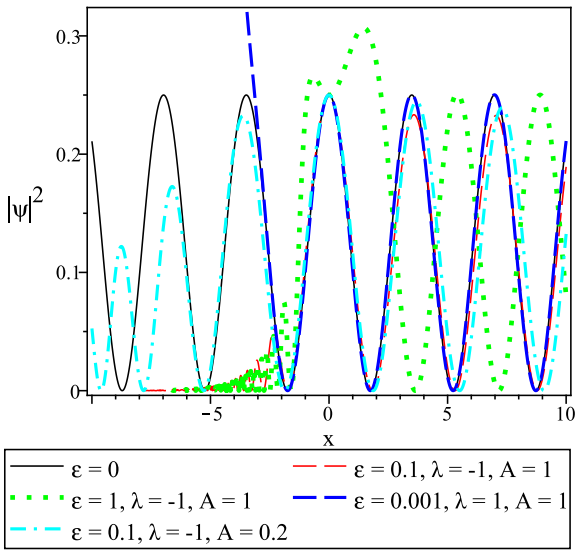

FIG. 7: (Color Online) Perturbations of the space-periodic sn-wave solution under the Morse potential $U(x) = \lambda\left(e^{-2Ax} - 2e^{-Ax}\right)$.

Morse potential is one example of an asymmetric trap [23, 24]. The Morse potential is given by $U(x) = \lambda\left(e^{-2Ax} - 2e^{-Ax}\right)$ where $\lambda > 0$ and $A > 0$. In contrast to the harmonic trap, the Morse potential increases more slowly along the positive x-axis. In relation to BECs, the Morse potential has previously been considered for models of trapped atoms [25].

For ease of computation, we set $A = \frac{\sqrt{2}}{2}$, which we may view as a scaling of x. This scaling makes the model approximately integrable in the case of $K^2 = 1$. Thus, taking $K^2 = 1$, we first compute the inner quantity of $\psi_1(x)$, finding

$$\begin{aligned}
&\int_0^y U(z)\psi_0(z)\psi_0{}'(z)\mathrm{d}z \\
&= \frac{\lambda}{\sqrt{2}}\int_0^y \frac{\left(e^{-2z/\sqrt{2}} - 2e^{-z/\sqrt{2}}\right)\left(e^{z/\sqrt{2}} - e^{-z/\sqrt{2}}\right)}{\left(e^{z/\sqrt{2}} + e^{-z/\sqrt{2}}\right)^3}\mathrm{d}z \\
&= \lambda\int_1^{e^{y/\sqrt{2}}} \frac{(\eta^{-2} - 2\eta^{-1})(\eta - \eta^{-1})}{(\eta + \eta^{-1})^3}\frac{\mathrm{d}\eta}{\eta} \\
&= \lambda\int_1^{e^{y/\sqrt{2}}} \frac{(1 - 2\eta)}{\eta(\eta^2+1)^2}\mathrm{d}\eta \\
&= \lambda\chi(e^{y/\sqrt{2}}) + \lambda\left(\frac{\pi+1}{4} - \ln\left(\frac{1}{\sqrt{2}}\right)\right),
\end{aligned} \tag{34}$$

where by χ we signify the function

$$\chi(\eta) = \ln\left(\frac{\eta}{\sqrt{\eta^2+1}}\right) - \tan^{-1}(\eta) - \frac{2\eta - 1}{2(\eta^2+1)}. \tag{35}$$

The first order perturbation theory is then given by

$$\begin{aligned}
\psi_1(x) &= \psi_0{}'(x)\int_0^x \frac{\lambda\chi(e^{y/\sqrt{2}}) + \lambda\left(\frac{\pi+1}{4} - \ln\left(\frac{1}{\sqrt{2}}\right)\right)}{\psi_0'(y)^2}\mathrm{d}y \\
&= \frac{\lambda}{\sqrt{2}}\psi_0{}'(x)\int_1^{e^{x/\sqrt{2}}}\left(\chi(\eta) + \left(\frac{\pi+1}{4} - \ln\left(\frac{1}{\sqrt{2}}\right)\right)\right) \\
&\qquad \times \frac{(\eta^2+1)^4}{\eta^5}\mathrm{d}\eta.
\end{aligned} \tag{36}$$

Simplifying this expression, we find

$$\begin{aligned}
\psi_1(x) = \frac{\lambda}{2}\Bigg\{&\Theta\left(e^{x/\sqrt{2}}\right) + \frac{2\ln 2 + \pi + 1}{8}\sinh(2\sqrt{2}x) \\
&- \frac{2}{3}\sinh\left(\frac{3x}{\sqrt{2}}\right) + \frac{4\ln 2 + 2\pi + 3}{2}\sinh(\sqrt{2}x) \\
&- 6\sinh\left(\frac{x}{\sqrt{2}}\right) - \frac{1}{8}e^{-2\sqrt{2}x} - \frac{1}{2}e^{-\sqrt{2}x} + \frac{5}{8} \\
&+ \frac{6\ln 2 + 6 + 3\pi}{2\sqrt{2}}x\Bigg\}\operatorname{sech}^2\left(\frac{x}{\sqrt{2}}\right),
\end{aligned} \tag{37}$$

where Θ denotes the integral

$$\Theta(\eta) = \int_1^\eta \left(\ln\left(\frac{\xi}{\sqrt{\xi^2+1}}\right) - \tan^{-1}(\xi)\right)\frac{(\xi^2+1)^4}{\xi^5}\mathrm{d}\xi. \tag{38}$$

We next consider the Morse potential for various values of A, and plot the perturbations of the sn-waves in Fig. 7, and perturbations of the dark soliton in Fig. 8. From Fig. 7, we see that perturbations to the sn-waves for small ϵ maintain much of the form of the sn-wave solution for $x > 0$. It is the $x > 0$ side of the Morse potential which is the weakest, so there is little forcing to disturb

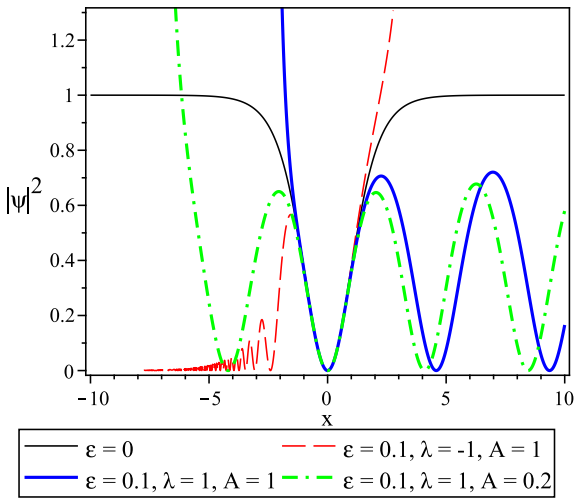

FIG. 8: (Color Online) Perturbations of the dark soliton solution corresponding to $K = 1$ under the Morse potential $U(x) = \lambda\left(e^{-2Ax} - 2e^{-Ax}\right)$.

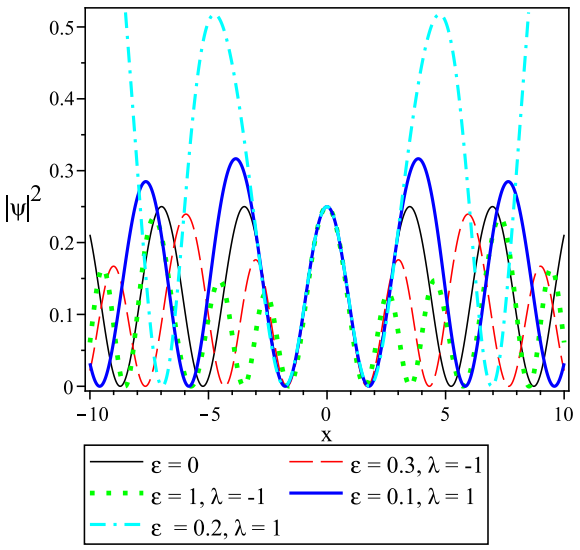

FIG. 9: (Color Online) Perturbations of the space-periodic sn-wave solution under the lattice potential $U(x) = \lambda\left(1 - \cos(x)\right)$.

the unperturbed form of the sn-wave. On the other hand, for $x < 0$, the space-periodic structure is destroyed, no matter the sign of λ. When $\lambda > 0$, the solution is confined to the right of the wall of the sharply increasing boundary of the potential. To the right of this boundary, the solution propagates as would a standard sn-wave. On the other hand, for the $\lambda < 0$ situation, the density rapidly decreases as x becomes larger in magnitude and negative. For larger values of ϵ, this effect is strengthened, and the larger ϵ solutions very rapidly decay. The strength of the asymmetric trapping potential decreases as we decrease the parameter A. As A decreases, the rate of decay of solutions corresponding to $\lambda < 0$ is slowed as $x \to -\infty$. For large ϵ, asymmetries can develop. For instance, in the $\epsilon = 1$ solution shown, the maximal density occurs at a positive value of x, and is never repeated (unlike the pure sn-wave, which exhibits density peaks at regular intervals).

Regarding the perturbations of the dark soliton solution, Fig. 8 demonstrates that the qualitative influence of the asymmetric potential is the same for the dark soliton perturbation theory. Indeed, for the $\lambda > 0$ case, the solutions are confined to the right of the stronger boundary. To the right of this boundary, the solutions exhibit properties of the sn-waves. The location of the boundary is shifted as the value of the parameter A is modified, however the general qualitative features of a perturbation is unchanged with A. In contrast, the solutions corresponding to $\lambda < 0$ are quite distinct in form from the solutions shown in Fig. 7. Here, the perturbations of the dark solutions in the $\lambda < 0$ case are confined to the left of the weaker boundary and diminish completely upon interacting with the stronger boundary. The effect is that these solutions have maximal density at the right end of the potential well, and oscillate while decreasing in average density toward the left end of the potential well.

G. Quantum pendulum potential: a lattice trap

The quantum pendulum potential takes the form $U(x) = \lambda\left(1 - \cos(x)\right)$, where $\lambda > 0$. This is a good model of an optical lattice type of potential, which has been used to study BECs in a number of settings [26]. $\psi_0(x)$ again remains as given in (10), but $U(x) = \lambda\left(1 - \cos(x)\right)$ in (15) results in $\psi_1(x)$ of the form

$$\psi_1(x) = \psi_0{}'(x) \int_0^x \frac{\int_0^y \lambda\left(1 - \cos(x)\right)\psi_0(z)\psi_0{}'(z)\,\mathrm{d}z}{\psi_0{}'(y)}\,\mathrm{d}y\,. \tag{39}$$

The $K^2 = 1$ condition, which offers the simplification $\psi_0(x) = \tanh\left(\frac{x}{\sqrt{2}}\right)$, allows for exact integration in $\psi_1(x)$. Thus the first order term reads

$$\begin{aligned}\psi_1(x) = \frac{\lambda}{576}\mathrm{sech}^2\left(\frac{x}{\sqrt{2}}\right)\Big\{&4\sin(x)\cosh\left(2\sqrt{2}x\right)\\ &+ 8\sqrt{2}\cos(x)\sinh\left(2\sqrt{2}x\right)\\ &-9\sqrt{2}\sinh\left(2\sqrt{2}x\right) - 36\sin(x) + 36x\Big\}\,.\end{aligned} \tag{40}$$

In performing this integration, we mention the use of the identity which takes $1 - \cos(x) = 1 - (\mathrm{e}^{ix} + \mathrm{e}^{-ix})/2$.

We next consider the pure lattice potential, and plot the perturbations of the sn-waves in Fig. 9, and perturbations of the dark soliton in Fig. 10. For both signs of λ, we obtain space-periodic solutions as perturbations of the pure sn-wave solutions, which exhibit radial symmetry about $x = 0$. The difference is that for $\lambda < 0$ the solutions decrease in overall density as ϵ increases, whereas for $\lambda > 0$ the solutions increase in overall density. Furthermore, and unlike previous cases considered, the oscillating solutions do not always show a tendency

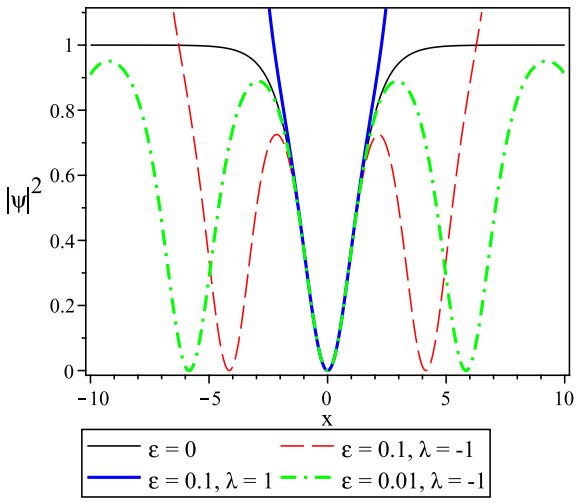

FIG. 10: (Color Online) Perturbations of the dark soliton solution corresponding to $K = 1$ under the lattice potential $U(x) = \lambda\,(1 - \cos(x))$.

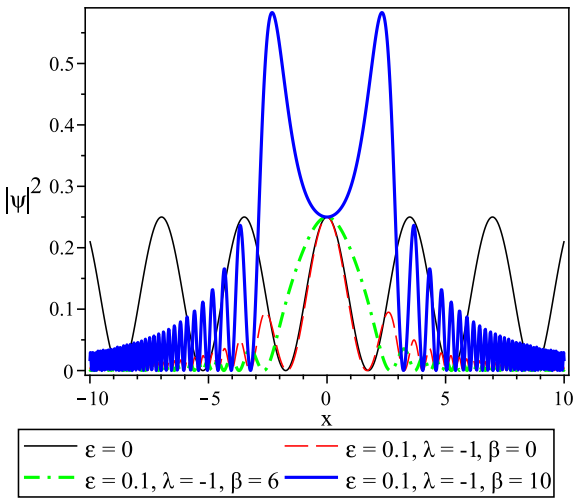

FIG. 11: (Color Online) Perturbations of the space-periodic sn-wave solution under the double-well potential $U(x) = \lambda[(x^2-1)^2 - \beta]$.

to decay as $|x|$ becomes large. Indeed, the solutions oscillate and exhibit density peaks which may increase over space. Solutions have a local density peak at $x = 0$, and then have symmetric secondary peaks. For $\lambda < 0$, these secondary peaks are of lower value than the peak at the origin, while for $\lambda > 0$ these secondary peaks are of higher density than at the origin. Furthermore, past the secondary peaks, some of the solutions have even larger peaks. The actual structure of these peaks appears strongly dependent on the value of the parameters and not just on their sign or relative magnitude.

Turning our attention to the perturbations of the dark soliton solutions shown in Fig. 10, we observe that for very small values of ϵ (of order 10^{-2} or less), the perturbation of the dark soliton results in an sn-wave type solution. Here the sn-wave has the property that its density is bounded above by the original tanh density curve of the dark soliton solution. However, increasing ϵ further into the 10^{-1} regime, we see that solutions (for both $\lambda > 0$ and $\lambda < 0$) are confined to near the origin, and do not pass beyond an inner well. In its region of existence, the $\lambda < 0$ solution exhibits oscillations, and closely approximates the dark soliton near $x = 0$. On the other hand, the $\lambda > 0$ solution exceeds the dark soliton solution, while also closely approximating the dark soliton near $x = 0$. So, for very small ϵ, the perturbed dark soliton collapses into an sn-wave solution.

H. Double-well potential

Various applications call for double-well potentials [27]. One possible form of such a potential used is $U(x) = \lambda[(x^2-1)^2 - \beta]$, which gives a simple and symmetric double-well. One may use the formulas in Section 3 to obtain the first order perturbation solution corresponding to a double-well potential. We omit the details here, and summarize the results. We consider the potential $U(x) = U(x) = \lambda[(x^2-1)^2 - \beta]$, and plot the perturbations of the sn-waves in Fig. 11, and perturbations of the dark soliton in Fig. 12.

Fig. 11 demonstrates that the perturbations of the sn-wave solution respond strongly to a change in the parameter β, which serves to shift the potential vertically. When $\beta = 0$, the small-ϵ solution matches the small-x density profile of the un-perturbed solution. However, as $|x|$ increases, note that the perturbed solution decays, with density tending toward zero. Increasing the value of β has the immediate effect of allocating more density near the origin, with less density present in the tails. Eventually, for large enough β, there is a qualitative change in the solution. Indeed, in the large-β regime, we see the formation of a double peak in density, present symmetrically on either side of the origin. The tails of these solutions decay as $|x|$ increases.

This type of bi-modal density distribution is particularly well pronounced when we consider the perturbation of the dark soliton solutions. Each perturbation solution obtained demonstrates symmetric peaks in density, on symmetric sides of the origin. As β increases, the density increases. This makes sense, as a decrease in β increases the well depth, permitting greater concentration of the density near the origin.

In all of the cases considered here, we have considered $\lambda < 0$. The $\lambda > 0$ case is strongly confined to the well, and is more or less like that discussed in the case of the harmonic potential.

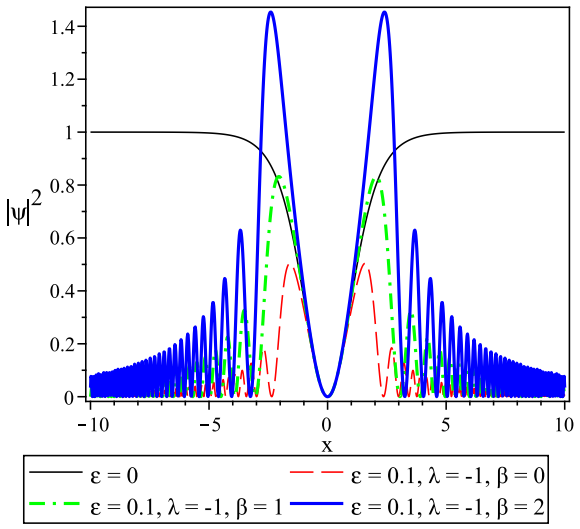

FIG. 12: (Color Online) Perturbations of the dark soliton solution corresponding to $K = 1$ under the double-well potential $U(x) = \lambda[(x^2 - 1)^2 - \beta]$.

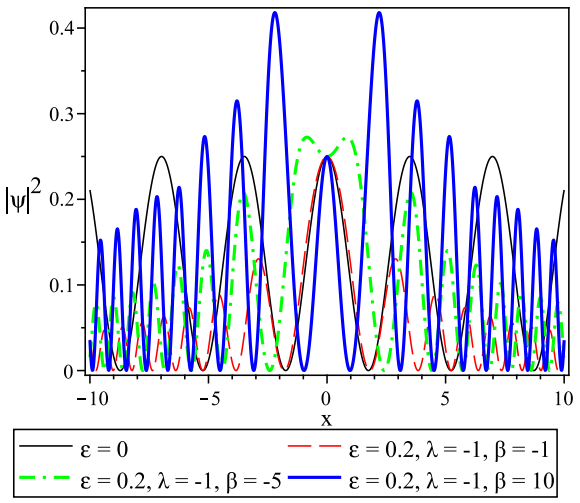

FIG. 13: (Color Online) Perturbations of the space-periodic sn-wave solution under the modified harmonic oscillator potential $U(x) = \lambda[x^2 + \beta\cos^2(x)]$.

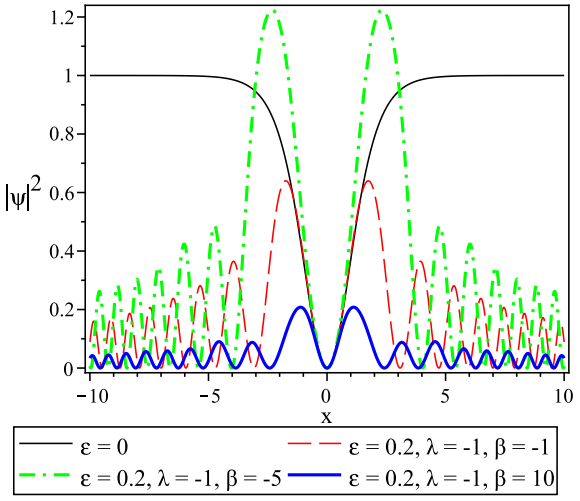

FIG. 14: (Color Online) Perturbations of the dark soliton solution corresponding to $K = 1$ under the modified harmonic oscillator potential $U(x) = \lambda[x^2 + \beta\cos^2(x)]$.

I. Harmonic potential with lattice trap

It is possible to combine a harmonic potential and lattice trap, or another combination of traps, to obtain pseudo or quasi periodic potentials, and this type of potential has been considered previously in differing settings [28].

One possible form of such a potential is $U(x) = \lambda[x^2 + \beta\cos^2(x)]$, which was used in [29]. This class of potential was shown to be useful for studying the 1D dynamics of a BEC of cold atoms in parabolic optical lattices [30]. We shall present some graphical results, but shall omit the detailed derivation of the perturbation solutions. Note that perturbation results can be obtained for a number of different types of lattice traps. We consider the potential $U(x) = \lambda[x^2 + \beta\cos^2(x)]$, since this potential is reasonably simple and has been considered elsewhere. We plot perturbations of the sn-waves in Fig. 13, and perturbations of the dark soliton in Fig. 14. Again, we shall only plot the $\lambda < 0$ case. The $\lambda > 0$ case is similarly behaved to the solutions obtained previously for the harmonic potential.

We see that the perturbations of the sn-waves decrease in amplitude for large x and continue this manner of decay as $|x|$ increases. The interesting differences occur close to the origin. For small ϵ and $\lambda < 0$, the solutions allocate more density near the origin as β is decreased, for negative β. Eventually, for β negative enough, we find that the distribution becomes bi-modal near the origin, with a single peak near the origin being replaced by a double peak which is symmetric with respect to the origin. On contrast, for large enough $\beta > 0$, we find a (relatively) small central peak at the origin, surrounded by two larger peaks on either side. These solutions then decay in average density as $|x|$ increases. So, the maximal density occurs either at the origin or in a pair of maxima on either side of the origin, depending on the value of β selected.

The situation changes somewhat when we consider perturbations of the dark solitons, as shown in Fig. 14. Indeed, perturbation solutions corresponding to either sign of β are similarly behaved, with density maxima spaced symmetrical on either side of the origin. It appears as though the total density is tied to the value of β. For larger magnitude, negative β, the density is rather largely congregated near the origin. For β near zero, the overall value of the density curve decreases, with oscillations still present. For large positive values of β, the density plot decreases further yet, and it appears as though the period between the oscillations is decreasing.

J. Elliptic function potentials: exactly solvable models

It was previously shown [4] that the potential

$$U(x) = \lambda \mathrm{sn}^2(x,k) \tag{41}$$

permits a closed form exact stationary solution. This is due in large part to the fact that the natural basis for the $\epsilon = 0$ problem can be given in terms of Jacobi elliptic functions. It is natural, then, to wonder if more complicated expressions can give similar results. To this end, it is tempting to consider an expansion of a potential in terms of Jacobi elliptic functions, say the potential

$$U(x) = \lambda_1 \mathrm{sn}^2(x,k) + \lambda_2 \mathrm{cn}^2(x,k) + \lambda_3 \mathrm{dn}^2(x,k)\,. \tag{42}$$

However, we quickly find that this cannot work, since we have no superposition principle (due to the cubic nonlinearity). We can, nonetheless, find solutions when two of the three λ's in (42) are zero. The $\lambda_2 = \lambda_3 = 0$ case is that considered in [4]. If we consider the $\lambda_1 = \lambda_3 = 0$ case, we have a potential

$$U(x) = \lambda_2 \mathrm{cn}^2(x,k)\,. \tag{43}$$

With such a potential we can obtain exact solutions in the form of one of $\psi(x) = A\mathrm{sn}(x,k)$, $\psi(x) = A\mathrm{cn}(x,k)$ or $\psi(x) = A\mathrm{dn}(x,k)$. For each choice, we obtain two algebraic conditions relating the amplitude A, the elliptic index k, and the parameter λ_2. First, when $\psi(x) = A\mathrm{sn}(x,k)$, we have the restrictions $A^2 = 2k^2 + \epsilon\lambda_2$ and $\epsilon\lambda_2 + k^2$. Thus, the solution takes the form

$$\psi(x) = \pm\sqrt{-\epsilon\lambda_2}\,\mathrm{sn}(x, \sqrt{-\epsilon\lambda_2})\,. \tag{44}$$

Assuming a solution $\psi(x) = A\mathrm{cn}(x,k)$, we have the conditions $A^2 + 2k^2 + \epsilon\lambda_2 = 0$ and $A^2 + \epsilon\lambda_2 = 0$, and hence $A = \sqrt{-\epsilon\lambda_2}$, $k = 0$, so

$$\psi(x) = \sqrt{-\epsilon\lambda_2}\,\mathrm{cn}(x,0) = \sqrt{-\epsilon\lambda_2}\cos(x)\,. \tag{45}$$

Finally, assuming a solution $\psi(x) = A\mathrm{dn}(x,k)$ we have the conditions $A^2k^2 + 2k^2 + \epsilon\lambda_2 = 0$ and $k^2 + A^2 + \epsilon\lambda_2 = 1$. Denote a solution k by

$$k_{\pm,\pm} = \pm\sqrt{\frac{3-\epsilon\lambda_2}{2} \pm \frac{1}{2}\sqrt{(3-\epsilon\lambda_2)^2 + 4\epsilon\lambda_2}}\,. \tag{46}$$

Then, we have four possible amplitudes:

$$A_{\pm,\pm} = \pm\sqrt{1 - \epsilon\lambda_2 - k_{\pm,\pm}^2}\,. \tag{47}$$

We therefore obtain possible solutions of the form

$$\psi(x) = A_{\pm,\pm}\mathrm{dn}(x, k_{\pm,\pm})\,. \tag{48}$$

For our final choice of potential, we consider the $\lambda_1 = \lambda_2 = 0$ case, so that we have the potential

$$U(x) = \lambda_3 \mathrm{dn}^2(x,k)\,. \tag{49}$$

First, assuming a solution $\psi(x) = A\mathrm{sn}(x,k)$, we find that $A^2 = -(2+\epsilon\lambda_3)\epsilon\lambda_3$ and $k^2 = -\epsilon\lambda_3$. Hence we have stationary solutions of the form

$$\psi(x) = \pm\sqrt{-(2+\epsilon\lambda_3)\epsilon\lambda_3}\,\mathrm{sn}(x, \pm\sqrt{-\epsilon\lambda_3})\,. \tag{50}$$

Next, assuming a solution $\psi(x) = A\mathrm{cn}(x,k)$, we find $A^2 = -\epsilon\lambda_3$ and $k^2 = \frac{\epsilon}{2+\epsilon\lambda_3}$, so our solution is

$$\psi(x) = \sqrt{-\epsilon\lambda_3}\,\mathrm{cn}\left(x, \sqrt{\frac{\epsilon}{2+\epsilon\lambda_3}}\right)\,. \tag{51}$$

Our final solution form is $\psi(x) = A\mathrm{dn}(x,k)$. Under this assumption, we have two sets of constraints: either $k^2 = 0$ and $A^2 = 1 - \epsilon\lambda_3$ or $k^2 = 3$ and $A^2 = -2 - \epsilon\lambda_3$. Therefore, we either have the solution

$$\psi(x) = \sqrt{1-\epsilon\lambda_3}\,\mathrm{dn}(x,0) = \sqrt{1-\epsilon\lambda_3} \tag{52}$$

(since $\mathrm{dn}(x,0) = 1$) or we have the solution

$$\psi(x) = \sqrt{-2-\epsilon\lambda_3}\,\mathrm{dn}(x, \pm\sqrt{3})\,. \tag{53}$$

V. CONCLUSIONS

We have shown that, by assuming a perturbation solution in the Jacobi elliptic function solution of the NLS equation with a free potential ($V(x) = 0$), one can construct accurate approximations for the NLS equation with non-trivial, though small, potential depending on space. In this way, we have obtained stationary solutions for the NLS equation with small yet arbitrary potential. Note that the solutions themselves need not be small, since such a requirement is unnecessary due to the assumption of a non-linear manner of perturbation, in which the order-zero perturbation solution is itself governed by a non-linear, rather than linear, differential equation. Subsequent terms in the perturbation expansion are governed by linear differential equations, and these added corrections to the order-zero term are small (whenever the solution is in the perturbative regime). When solutions are in the perturbative regime, we can apply the general method outlined in Section 3 in order to determine the influence of the addition of a small potential on the order-zero elliptic function solutions.

In the case where the potential is either constant or an elliptic function, we obtain exact solutions. When the potential is zero, we have the class of dark soliton solutions of the form

$$\Psi(x,t) = 2\hbar\sqrt{\frac{m}{g}}\exp\left(-4i\hbar m t\right)\tanh\left(\frac{x}{\sqrt{2}}\right)\,,$$

which is the standard soliton solution for the repulsive BEC. In the case of a non-zero yet constant potential, or a potential expressed in terms of Jacobi elliptic functions, we find that the space dependence of a stationary solution scales as a Jacobi elliptic function. The case of elliptic

potentials is in complete agreement with the results of [4], where a Jacobi sn elliptic potential was considered. In the present paper, we have reported similar results for the case of potentials involving Jacobi cn or dn functions.

For the remainder of the potentials given, the perturbation expansions do not terminate to give exact solutions. However, for small potentials (which we model as small ϵ), we obtain reasonably accurate perturbation solutions at first or second order. This permits us to study a number of different potentials resulting in the solutions of NLS equations where exact methods necessarily fail. While the perturbation results here assume a zeroth-order solution in terms of a Jacobi sn function, note that we could have considered zeroth-order solutions in the form of Jacobi cn or dn elliptic function. The solution methods for each would be analogous to those presented here for the Jacobi sn case.

In the case where the elliptic function parameter K satisfies $K^2 = 1$, the Jacobi elliptic sn functions reduce to hyperbolic tangent functions, so in this case the perturbation results determine the first order (and second order, where used) perturbation theories for the one-soliton solution of a repulsive BEC under a small potential. In the case of an attractive BEC ($g < 0$), we can obtain similar results, where the perturbation is performed with respect to the order-zero solution

$$\Psi(x,t) = 2\hbar\sqrt{-\frac{m}{g}}\exp\left(-4i\hbar mt\right)\mathrm{sech}\left(\frac{x}{\sqrt{2}}\right),$$

which is simply the one-soliton arising in the attractive BEC situation with a free potential. Additional solutions are also possible for the attractive BEC, and the study of the NLS with arbitrary small potentials in the attractive case is another possible area of future work. While the general method will be like that outlined here, there will be certain fundamental qualitative differences in the solutions.

While we have considered a number of potentials here, our list of potentials is far from exhaustive. That said, for any reasonable small potential, the methods outlined here can be applied. Therefore, our elliptic function perturbation approach can allow one to study NLS equations which model the influence of any number of choices of confining potentials for BECs. In principle, one may construct higher order perturbation theories, but in order to obtain qualitatively reasonable results often the first order perturbation results are sufficient. The method can also be coupled with numerical methods. Indeed, one can assume an elliptic function solution for the order-zero perturbation solution, and then obtain a successive system of equations for the higher-order terms. Since each of these higher order equations are linear, one may apply a numerical routine to solve these equations. In this way, one may numerically determine the higher order corrections to the stationary solutions without the convoluted higher order terms.

Note that it is also possible to consider potentials of the form $1/x^\alpha$. However, if $\alpha > 2$, the solution to the NLS can develop a non-removable singularity at the origin. In such a case, one should consider a non-local formulation of the model. Either way, note that the perturbation results here would be expected to break down for such potentials, owing to the forced non-locality inherent in dealing with such potentials which become arbitrarily large near the origin.

It should also be mentioned that the results here can be carried over to the scenario in which there are more than one space dimensions. In this case, the stationary solution is determined exactly by a solution to the PDE

$$\triangle\psi + (1 - \epsilon U(\mathbf{x}))\psi - \psi^3 = 0\,. \tag{54}$$

If one can obtain a solution to the $\epsilon = 0$ non-linear equation $\triangle\psi + \psi - \psi^3 = 0$, then in principle, one may use a method similar to that outlined here to construct a perturbation solution which will give higher order linear corrections due to the potential U.

Regarding another area of future work, it is possible to study the stability of these types of dark soliton or sn-wave solutions. The stability or instability of these kinds of stationary states can be determined through an application of the VK stability criteria [31]. It would be particularly interesting to consider the orbital stability of the sn-wave solutions. Recently, the stability of these types of solutions has been considered for other integrable models admitting sn-wave type solutions, such as the integrable WKIS [32] and LIA [33] models.

Acknowledgements

R.A.V. supported in part by NSF grant # 1144246. The authors appreciate the comments of a reviewer which have led to improvement in the paper.

[1] F. Dalfovo, S. Giorgini, L. P. Pitaevskii, and S. Stringari, Rev. Mod. Phys. 71, 463 (1999); [2] L. D. Carr, M. A. Leung, and W. P. Reinhardt, J. Phys. B: At. Mol. Opt. Phys. 33, 3983 (2000); M. Key et al., Phys. Rev. Letts. 84, 1371 (2000); N. H. Dekker et al., Phys. Rev. Letts. 84, 1124 (2000).

[2] M. Kunze and et. al, Physica D 128, 273 (1999); Y. S. Kivshar, T. J. Alexander, and S. K. Turitsyn, Phys. Lett. A 278, 225 (2001)

[3] S. Theodorakis and E. Leontidis, J. Phys. A 30, 4835 (1997); F. Barra, P. Gaspard, and S. Rica, Phys. Rev. E 61, 5852 (2000).

[4] J. C. Bronski, L. D. Carr, B. Deconinck, and J. N. Kutz, Phys. Rev. Lett. 86 (2001) 1402.

[5] B. P. Anderson and M. A. Kasevich, Science 282, 1686 (1998); E. W. Hagley et al., Science 283, 1706 (1999).

[6] Y. B. Ovchinnikov et al., Phys. Rev. Lett. 83, 284 (1999).

[7] D. Jaksch et al., Phys. Rev. Lett. 81, 3108 (1998); G. K. Brennen, C. M. Caves, P. S. Jessen, and I. H. Deutsch, Phys. Rev. Lett. 82, 1060 (1999).

[8] D.-I. Choi and Q. Niu, Phys. Rev. Letts. 82, 2022 (1999).

[9] E.M. Lifshitz and L.P. Pitaevskii, Statistical Physics Part 2: Landau and Lifshitz course of Theoretical physics, Butterworth-Heinemann (1980).

[10] L. D. Carr, C. W. Clark, and W. P. Reinhardt, Phys. Rev. A 62, 063610 (2000).

[11] L. D. Carr, C. W. Clark, and W. P. Reinhardt, Phys. Rev. A 62, 063611 (2000).

[12] J.C. Bronski, L. D. Carr, B. Deconinck, J. N. Kutz, and K. Promislow, Phys. Rev. E 63, 036612 (2001).

[13] X.-F. Zhou, S.-L. Zhang, Z.-W. Zhou, B. A. Malomed, and H. Pu, Phys. Rev. A 85, 023603 (2012).

[14] H. Cartarius and G Wunner, Phys. Rev. A 86, 013612 (2012).

[15] R D'Agosta and C Presilla, Phys. Rev. A 65, 043609 (2002).

[16] R. A. Van Gorder, J. Fluid Mech. 707, 585 (2012); R.A. Van Gorder, Prog. Theor. Phys. 128, 993 (2012); R. A. Van Gorder, Phys. Rev. E 86, 057301 (2012).

[17] R.-J. Lange, Journal of High Energy Physics 2012 (2012) 1.

[18] W. van Dijk and K. A. Kiers, Am. J. Phys. 60 (1992) 520; T.C. Scott, J.F. Babb, A. Dalgarno and J. D. Morgan III, J. Chem. Phys. 99 (1993) 2841.

[19] N. Regnault, T. Jolicoeur, Phys. Rev. Lett. 91 (2003) 030402.

[20] F. Dalfovo, S. Giorgini, L.P. Pitaevskii, S. Stringari, Rev. Mod. Phys. 71 (1999) 463; Z. X. Liang, Z. D. Zhang, W. M. Liu, Phys. Rev. Lett. 94 (2005) 050402; S. K. Adhikari, Phys. Rev. E 62 (2000) 2937-2944; V. M. Pérez-García, H. Michinel, J. I. Cirac, M. Lewenstein, P. Zoller, Phys. Rev. A 56 (1997) 1424; W. Bao, D. Jaksch, P. A. Markowich, J. Comput. Phys. 187 (2003) 318.

[21] G. Theocharis, Z. Rapti, P.G. Kevrekidis, D.J. Frantzeskakis, V.V. Konotop, Phys. Rev. A 67 (2003) 063610.

[22] M. Landtman, Phys. Lett. A 175 (1993) 147; A. L. Fetter, Phys. Rev. A 64 (2001) 063608

[23] P.M. Morse, Phys. Rev. 34 (1929) 57-64.

[24] Y. Zhou, M. Karplus, K.D. Ball, R.S. Bery, J. Chem. Phys 116 (2002) 2323-2329.

[25] W. C. Stwalley, L. H. Nosanow, Phys. Rev. Lett. 36 (1976) 910; B. D. Esry, C. H. Greene, Phys. Rev. A 60 (1999) 1451

[26] S. Burger, F. S. Cataliotti, C. Fort, F. Minardi, M. Inguscio, M. L. Chiofalo, M. P. Tosi, Phys. Rev. Lett. 86 (2001) 4447; M. Greiner, I. Bloch, O. Mandel, T.W. Hänsch, Phys. Rev. Lett. 87 (2001) 160405; M. Greiner, O. Mandel, T. W. Hänsch, I. Bloch, Nature 419 (2002) 51; C. Orzel, A. K. Tuchman, M. L. Fenselau, M. Yasuda, M. A. Kasevich, Science 291 (2001) 2386; S. Burger, F. S. Cataliotti, C. Fort, F. Minardi, M. Inguscio, M. L. Chiofalo, M. P. Tosi, Phys. Rev. Lett. 86 (2001) 4447; G. Chong, W. Hai, Q. Xie, Phys. Rev. E 70 (2004) 036213.

[27] G. J. Milburn, J. Corney, E. M. Wright, D. F. Walls, Phys. Rev. A 55 (1997) 4318; Y. Shin, M. Saba, T. A. Pasquini, W. Ketterle, D. E. Pritchard, A. E. Leanhardt, Phys. Rev. Lett. 92 (2004) 050405; A. Smerzi, S. Fantoni, S. Giovanazzi, S. R. Shenoy, Phys. Rev. Lett. 79 (1997) 4950; L. Pitaevskii, S. Stringari, Phys. Rev. Lett. 87 (2001) 180402; J. Ruostekoski, D. F. Walls, Phys. Rev. A 58 (1998) R50; R. W. Spekkens, J. E. Sipe, Phys. Rev. A 59 (1999) 3868; K. W. Mahmud, H. Perry, W. P. Reinhardt, Phys. Rev. A 71 (2005) 023615

[28] G. Roati et al., Nature 453 (2005) 895; F. S. Cataliotti, L. Fallani, F. Ferlaino, C. Fort, P. Maddaloni, M. Inguscio, New J. Phys. 5 (2003) 71; A. Smerzi, A. Trombettoni, Phys. Rev. A 68 (2003) 023613; K. J. H. Law, P. G. Kevrekidis, B. P. Anderson, R. Carretero-González, D. J. Frantzeskakis, J. Phys. B: At. Mol. Opt. Phys. 41 (2008) 195303

[29] L. Fallani, L. De Sarlo, J. E. Lye, M. Modugno, R. Saers, C. Fort, M. Inguscio, Phys. Rev. Lett. 93 (2004) 140406

[30] J. Brand, A. R. Kolovsky, European Physical Journal D 41 (2007) 331.

[31] M.G. Vakhitov and A.A. Kolokolov, Sov. Radiophys. 16 (1973) 783.

[32] R.A. Van Gorder, J. Phys. Soc. Japan 82 (2013) 064005.

[33] R.A. Van Gorder, J. Phys. Soc. Japan (2013), in press.